Title

Cell-to-cell interaction requires optimal positioning of a pilus tip adhesin modulated by gram-positive transpeptidase enzymes

Journal

Proceedings of the National Academy of Sciences of the United States of America, 116(36)

ISSN

0027-8424

Authors

Chang, Chungyu
Wu, Chenggang
Osipiuk, Jerzy
et al.

Publication Date

2019-09-03

DOI

10.1073/pnas.1907733116

Peer reviewed

Cell-to-cell interaction requires optimal positioning of a pilus tip adhesin modulated by gram-positive transpeptidase enzymes

Chungyu Chang[a,1,2], Chenggang Wu[b,1], Jerzy Osipiuk[c,d], Sara D. Siegel[b], Shiwei Zhu[e], Xiangan Liu[b], Andrzej Joachimiak[c,d], Robert T. Clubb[f], Asis Das[g], and Hung Ton-That[a,h,2]

[a]Division of Oral Biology and Medicine, School of Dentistry, University of California, Los Angeles, CA 90095; [b]Department of Microbiology & Molecular Genetics, University of Texas Health Science Center, Houston, TX 77030; [c]Center for Structural Genomics of Infectious Diseases, Consortium for Advanced Science and Engineering, University of Chicago, Chicago, IL 60637; [d]Structural Biology Center, Argonne National Laboratory, Lemont, IL 60439; [e]Department of Microbial Pathogenesis, Yale School of Medicine, New Haven, CT 06510; [f]Department of Chemistry and Biochemistry, University of California, Los Angeles–Department of Energy Institute of Genomics and Proteomics, University of California, Los Angeles, CA 90095; [g]Department of Medicine, Neag Comprehensive Cancer Center, University of Connecticut Health Center, Farmington, CT 06030; and [h]Molecular Biology Institute, University of California, Los Angeles, CA 90095

Edited by Scott J. Hultgren, Washington University School of Medicine in St. Louis, St. Louis, MO, and approved July 30, 2019 (received for review May 3, 2019)

Assembly of pili on the gram-positive bacterial cell wall involves 2 conserved transpeptidase enzymes named sortases: One for polymerization of pilin subunits and another for anchoring pili to peptidoglycan. How this machine controls pilus length and whether pilus length is critical for cell-to-cell interactions remain unknown. We report here in *Actinomyces oris*, a key colonizer in the development of oral biofilms, that genetic disruption of its housekeeping sortase SrtA generates exceedingly long pili, catalyzed by its pilus-specific sortase SrtC2 that possesses both pilus polymerization and cell wall anchoring functions. Remarkably, the *srtA*-deficient mutant fails to mediate interspecies interactions, or coaggregation, even though the coaggregation factor CafA is present at the pilus tip. Increasing ectopic expression of *srtA* in the mutant progressively shortens pilus length and restores coaggregation accordingly, while elevated levels of shaft pilins and SrtC2 produce long pili and block coaggregation by SrtA$^+$ bacteria. With structural studies, we uncovered 2 key structural elements in SrtA that partake in recognition of pilin substrates and regulate pilus length by inducing the capture and transfer of pilus polymers to the cell wall. Evidently, coaggregation requires proper positioning of the tip adhesin CafA via modulation of pilus length by the housekeeping sortase SrtA.

pilus length | coaggregation | sortase | gram-positive bacteria | pilus assembly

Pili or fimbriae are multicomponent protein polymers produced by both gram-negative and gram-positive bacteria that extend beyond the bacterial cell envelope and take part in many important processes, including DNA transport, motility, polymicrobial interactions or coaggregation, biofilm formation, and bacterial adherence to host tissues or abiotic surfaces (1, 2). Pili vary in length, ranging from a few hundred nanometers to several micrometers; for example, long pili of more than 4 μm are produced by many nonpathogenic and pathogenic *Neisseria*, while short pili, 175 to 210 nm in length, were only observed in nonpathogenic *Neisseria* (3). *Porphyromonas gingivalis*, however, assembles both long and short fimbriae critical for bacterial coaggregation and colonization (4). How various pilus lengths influence cell-to-cell interactions is not well understood, although it has been suggested that long pili might promote long-distance contacts, while short pili and cell wall-linked pilins enable intimate associations (5).

Unique to gram-positive bacteria are covalently linked pili, which also vary in length (6, 7) and are anchored to bacterial peptidoglycan by a conserved transpeptidase enzyme termed sortase (5, 8). A large number of gram-positive bacteria, including *Actinomyces* spp., *Corynebacterium diphtheriae*, *Bacillus cereus*, *Enterococcus faecalis*, and many streptococcal species (7, 9–15), employ a specialized sortase enzyme, called pilus-specific sortase or class C sortase, to polymerize individual pilin subunits into proteinaceous fibers; cell wall anchoring of these polymers is subsequently catalyzed by class A or class E sortases (16–20). The classification of sortases (A to F) is based on the sortase recognition motif located in the C-terminal cell wall sorting signal of substrate proteins, clustering of substrate and sortase genes, structural configurations of sortase enzymes, and their presumed functions (21, 22). Class A sortases, like the archetypal sortase A of *Staphylococcus aureus*, recognize an LPXTG motif of the C-terminal cell wall sorting signal in the substrate proteins (23), whereas class E sortases, such as SrtF of *C. diphtheriae* and SrtE1 of *Streptomyces coelicolor*, prefer an LAXTG motif (16, 24, 25). In addition to recognizing the LPXTG motif present in most pilins, class C sortases recognize the reactive lysine residue within the pilin motif of major pilus subunit proteins (26), thereby cross-linking individual pilins via the threonine-lysine isopeptide bond (27). It is noteworthy that most gram-positive bacteria also encode a large number of surface proteins that are

Significance

Covalently linked pili are produced by many gram-positive bacteria; these heteropolymers in various lengths are assembled on the bacterial peptidoglycan by conserved cysteine transpeptidase enzymes named sortases. How the sortase machine controls pilus length and whether pilus length is crucial for bacterial interactions remain elusive. We discover herein that the housekeeping sortase of *Actinomyces oris* utilizes 2 structural elements for recognition of pilin substrates to control pilus length, hence positioning of pilus tip adhesins. Importantly, we show that optimal positioning of pilus tip adhesins is critical for interspecies interactions, or coaggregation, a prerequisite for the development of oral biofilms.

Author contributions: C.C., C.W., J.O., A.J., A.D., and H.T.-T. designed research; C.C., C.W., J.O., S.D.S., S.Z., and X.L. performed research; C.C., C.W., J.O., S.D.S., S.Z., X.L., A.J., R.T.C., A.D., and H.T.-T. analyzed data; and C.C., C.W., J.O., R.T.C., A.D., and H.T.-T. wrote the paper.

The authors declare no conflict of interest.

This article is a PNAS Direct Submission.

Data deposition: Atomic coordinates and structure factors have been deposited into the Protein Data Bank, www.pdb.org (PDB ID code 5UTT).

[1]C.C. and C.W. contributed equally to this work.

[2]To whom correspondence may be addressed. Email: jchang@dentistry.ucla.edu or htonthat@dentistry.ucla.edu.

This article contains supporting information online at www.pnas.org/lookup/suppl/doi:10.1073/pnas.1907733116/-/DCSupplemental.

Published online August 19, 2019.

substrates of class A and E sortases (21, 28), suggesting that there is a hierarchy of substrate specificity. It remains unclear how these sortase enzymes partake in pilus assembly while performing a housekeeping function (i.e., cell wall anchoring of all other surface proteins), especially for class E sortases, with the majority of substrate proteins possessing an LAFTG motif like sortase A of *Actinomyces oris* (29).

A. oris produces 2 distinct types of pili or fimbriae. Type 1 fimbriae are composed of the shaft pilin FimP and the tip adhesin FimQ, which mediates bacterial adherence to the salivary proline-rich proteins (PRPs) that coat the tooth surface (30, 31). Type 2 fimbriae are made of the shaft pilin FimA and the tip pilin FimB (9, 32). FimA also forms a distinct pilus structure with another tip pilin named CafA, genetically unlinked to the fimbrial gene cluster; CafA is essential for polymicrobial interactions, termed coaggregation, as *A. oris cafA* mutant cells are unable to interact with *Streptococcus oralis* (29). While all Fim pilins contain a C-terminal LPXTG motif, the shaft pilins FimA and FimP also possess a pilin motif (9, 29). Polymerization of individual pilins into a covalently linked structure requires a pilus-specific sortase: That is, SrtC1 and SrtC2 for type 1 and type 2 fimbriae, respectively (9, 30). In *A. oris*, it has been suggested that the housekeeping sortase SrtA, predicted to be a class E sortase (21), is involved in cell wall anchoring of pilus polymers (33). Surprisingly, in *A. oris srtA* is an essential gene, unlike any other sortase genes studied to date (34). A forward genetic screen by Tn5 transposon mutagenesis led to the discovery that the loss of bacterial viability in the absence of the housekeeping sortase is linked to the cell wall-anchored glycoprotein GspA, which accumulates within and crowds the cytoplasmic membrane when *srtA* is genetically disrupted, thereby leading to cell envelope stress and ultimately cell death (34). Curiously, all *srtA* suppressor mutants isolated so far, including *gspA*, produce unusually long pili and are defective in interspecies interactions (34). This has led us to hypothesize that the housekeeping sortase SrtA is involved in modulating pilus length, and in turn, bacterial coaggregation.

Here, we report the molecular, structural, and physiological characterizations of the housekeeping sortase SrtA of *A. oris*. We demonstrate that the spatial positioning of the pilus tip adhesin CafA at an optimum distance away from the cell surface is critical for bacterial coaggregation and that SrtA plays an essential role in governing the optimal pilus length that dictates CafA spatial positioning. Our structural genetic studies identified 2 conserved structural elements of SrtA, the Y131 residue and the GVN motif, mutations of which, respectively, decrease and increase the pilus length and affect coaggregation positively and negatively. Molecular characterizations support the idea that these elements are required for the hierarchal recognition of SrtA substrates, hence controlling pilus polymerization and cell wall anchoring catalyzed by sortase enzymes. Given that sortase-mediated pilus assembly is conserved in gram-positive bacteria, our studies provide a paradigm of how a sortase machine mechanistically assemble adhesive pili with optimal length that is critical for cell-to-cell adherence.

Results

Genetic Disruption of the *A. oris* Housekeeping Sortase Generates Extensively Long Fimbriae on the Bacterial Surface That Fail to Mediate Polymicrobial Interactions. As mentioned above, all genetic suppressors of lethality of the *A. oris* Δ*srtA* mutant, irrespective of the nature of the Tn5-inactivated suppressor gene, produce unusually long fimbriae (34), suggesting that the housekeeping sortase plays a vital role in controlling pilus length. To test this, we began our studies using the double-mutant Δ*gspA*/Δ*srtA*, in which the viability of Δ*srtA* was regained by the removal of the glycoprotein GspA, whose toxic accumulation in the cytoplasmic membrane in the absence of SrtA would otherwise trigger cell envelope stress and subsequently cell death (34). To characterize the fimbriae produced, *A. oris* mutant cells were first examined by electron microscopy with negative staining. As expected, the *gspA* mutant with intact SrtA assembled fimbriae with average length comparable to that of the parental strain MG1, whereas the Δ*gspA*/Δ*srtA* double mutant produced abnormally long fimbriae (Fig. 1 *A–C*). Complementation by constitutive expression of *srtA* from a plasmid in this double mutant restored fimbrial length to the wild-type level (Fig. 1*D*).

As mentioned, *A. oris* MG1 assembles 2 antigenically distinct pili known as type 1 and type 2 fimbriae (9, 30, 32). To determine if both fimbrial types are affected by *srtA* deletion, we labeled cells separately with antibodies specific for the pilus shaft of type 1 (α-FimP) and type 2 fimbriae (α-FimA), followed by staining with IgG-conjugated gold particles and analyzed by electron microscopy (IEM). The pilus phenotypes revealed by immunogold labeling in the Δ*gspA* and Δ*gspA*/Δ*srtA* mutant strains, as well as the complemented Δ*gspA*/Δ*srtA*/pSrtA strain, affirmed the negative staining results (Fig. 1 *E–I*). Together, these results strengthen the notion that SrtA is a critical determinant of the proper assembly of both fimbriae with typical lengths observed in the wild-type cells.

The type 2 fimbriae are essential for *A. oris* coaggregation with other oral bacteria, a process crucial for oral biofilm development (29). Therefore, we asked if atypically long fimbriae that the *srtA*-deficient cells produced are still able to mediate bacterial coaggregation normally. We monitored coaggregation using an established assay (35), mixing cells of various *A. oris* strains with *S. oralis* (So34) in equal numbers in microtiter plates and incubating for a brief period before visual inspection, imaging, and quantification. As reported in our previous work, coaggregation was abrogated by deletion of either *fimA* that makes up the pilus shaft or *cafA*, a noncanonical tip adhesin of type 2 fimbriae (29) (*SI Appendix*, Fig. S1*A*; compare MG1 with Δ*cafA* and Δ*fimA*). The mutant cells devoid of *gspA* were able to aggregate with *S. oralis* at levels comparable to wild-type MG1 cells (*SI Appendix*, Fig. S1*A*, strain Δ*gspA*), demonstrating that GspA plays no role in coaggregation. Strikingly, no coaggregation was observed in the Δ*gspA*/Δ*srtA* mutant, while constitutive expression of *srtA* in this mutant rescued the coaggregation defect (*SI Appendix*, Fig. S1*A*, last 2 strains). The same set of strains was then analyzed for their ability to form FimA-dependent biofilms following methods we previously described (32). In sharp contrast to the coaggregation defect of the Δ*srtA* mutant, no significant defects in biofilm formation were apparent in strains lacking *gspA* alone or both *gspA* and *srtA*, as compared to the MG1 and Δ*cafA* strains (*SI Appendix*, Fig. S1*B*). Thus, the housekeeping sortase is dispensable for formation of *Actinomyces* monospecies biofilms.

A Critical Positional Role of the Pilus Tip in Interspecies Interactions. As presented above, cells displaying abnormally long FimA fimbriae in the absence of SrtA form biofilms, but they somehow fail to mediate interspecies interactions. Because CafA is the major coaggregation factor associated with the FimA-containing fimbriae (29), the failure of the Δ*gspA*/Δ*srtA* mutant to coaggregate with *S. oralis* might be attributed to the lack of CafA on the pilus tip and the bacterial surface. Alternatively, it is conceivable that excessive extension of pilus effectively misplaces the tip adhesive CafA away from the cell envelope that hinders a productive cell-to-cell interaction. To distinguish these scenarios, we first analyzed surface assembly of CafA by IEM. The data showed that while the tip-localized CafA was abundantly displayed in the parental MG1 strain, it was absent in the Δ*cafA* mutant, as expected; moreover, in the *fimA* mutant that lacked pili, CafA was still observed on the bacterial surface (*SI Appendix*, Fig. S1 *C–E*). Similar tip localization and abundance of CafA was seen in the Δ*gspA* strain (*SI Appendix*, Fig. S1*F*).

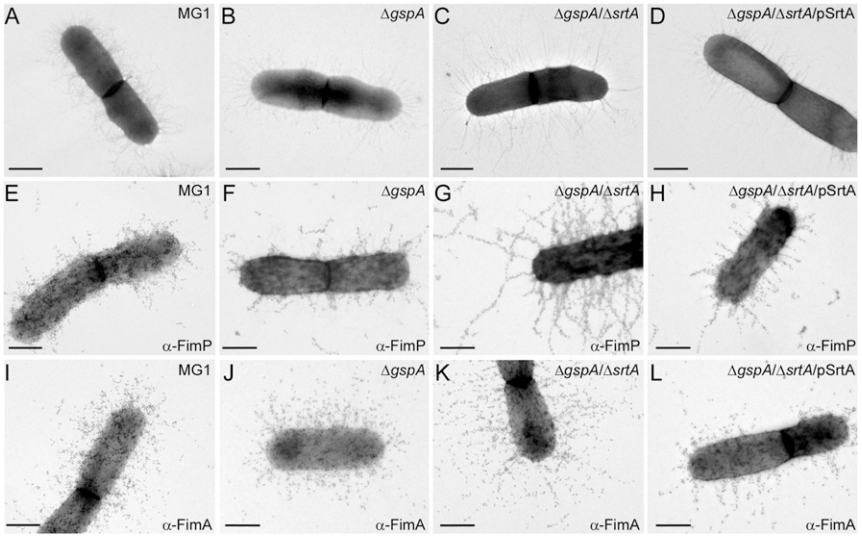

Fig. 1. *srtA*-deficient cells assemble exceedingly long pili. (*A–D*) Cells of *A. oris* strains were immobilized on carbon-coated nickel grids and directly stained with 1% uranyl acetate prior viewing by an electron microscope. For immunogold labeling (*E–L*), immobilized cells on grids were stained with antibodies against FimP (type 1 fimbriae) (*E–H*) or FimA (type 2 fimbriae) (*I–L*), followed by 12-nm colloidal gold particles conjugated with IgG. (Scale bars, 0.5 μm.)

Notably, in the Δ*gspA*/Δ*srtA* mutant, most gold particle-labeled CafA at the pilus tips appeared to be positioned much farther away from the cell surface (*SI Appendix*, Fig. S1*G*). Constitutive expression of SrtA from a plasmid in this strain reduced this aberrant positioning of CafA (*SI Appendix*, Fig. S1*H*). Therefore, the coaggregation defect in the absence of SrtA is not due to the lack or reduction of CafA at pilus tips. Rather, it might be due to the abnormal location of CafA.

To firmly establish this point, we quantified the relative abundance of surface CafA by whole-cell ELISA, as previously reported (36). Compared to the MG1 strain, the Δ*fimA* mutant displayed 3-fold reduction in net CafA signal (*SI Appendix*, Fig. S1*I*, first and third columns). Deletion of *gspA* caused a slight decrease in surface CafA (*SI Appendix*, Fig. S1*I*, column Δ*gspA*), but this mutant strain was still able to aggregate with *S. oralis* (*SI Appendix*, Fig. S1*A*). Strikingly, the Δ*gspA*/Δ*srtA* mutant and its complemented strain displayed similar levels of surface CafA as compared to that of MG1 (*SI Appendix*, Fig. S1*I*, last 2 columns), yet the former was coaggregation-negative and the latter coaggregation-positive (*SI Appendix*, Fig. S1*A*). To explore if overexpression of CafA in the Δ*gspA*/Δ*srtA* double mutant rescues its coaggregation defect, we introduced into this strain a multicopy plasmid-expressing CafA under the control of a constitutive promoter (pCafA) (29), and coaggregation was quantitatively determined as described before (37). Compared to the MG1 strain, which coaggregation efficiency was normalized to 1, overexpression of CafA could not rescue the coaggregation defect of the Δ*gspA*/Δ*srtA* mutant (*SI Appendix*, Fig. S2).

Next, to estimate the relative change in the distance of CafA from the cell surface, cells from the MG1 and Δ*gspA*/Δ*srtA* strains were subjected to IEM using α-CafA antibodies and IgG-conjugated gold particles (*SI Appendix*, Fig. S1*C*). Representative IEM images were then analyzed by drawing circumferential outlines of CafA-labeled gold particles and determining the linear distance between the outlines and the cell envelope at various locations were determined by ImageJ (https://imagej.nih.gov/ij/). Indeed, as shown in *SI Appendix*, Fig. S3 *A–C*, the average distance of CafA from the cell envelope increased more than 6-fold in the Δ*gspA*/Δ*srtA* mutant (1.55 ± 0.15 μm) as compared to that of the MG1 strain (0.25 ± 0.04 μm). Because the IEM procedure involves multiple steps that could artificially alter fimbrial length, we independently determined the type 2 fimbrial length by cryoelectron tomography (cryo-ET), using strains lacking the type 1-specific sortase SrtC1 (Δ*srtC1*) and hence devoid of the type 1 fimbriae. In this procedure, *A. oris* cells on grids were plunge-frozen into liquid ethane to preserve their native state. A series of tilt images of type 2 fimbriae were collected, and reconstruction of tilt series into tomogram and modeling were performed by the IMOD software package (38) (*Materials and Methods*). In agreement with the IEM results, the SrtA$^-$ strain (Δ*gspA*/Δ*srtA*/Δ*srtC1*) produced extended fimbriae averaging up to 1.85 μm that are 3 times longer than those in the SrtA$^+$ strain (Δ*srtC1*) (*SI Appendix*, Fig. S3*D*) (compare 1.85 ± 0.53 μm to 0.58 ± 0.88 μm).

Taken together, these results demonstrate that in the absence of SrtA, sufficient amounts of CafA$^+$ pili, which are 3 times longer, are assembled and surface anchored in *A. oris*. This leads us to posit that the coaggregation defect caused by the absence of SrtA is due to the extended distance of the coaggregation mediator CafA from the cell surface.

Pilus-Specific Sortase SrtC2 Catalyzes Pilus Polymerization and Cell Wall Anchoring of Pilus Polymers. The findings above appear to be incongruent with previous studies that substantiate the role of the housekeeping sortase in cell wall anchoring of pili in many gram-positive bacteria, including *C. diphtheriae*, *B. cereus*, *E. faecalis*, and *Streptococcus agalactiae*; in these organisms, deletion of the housekeeping sortase gene results in pilus shedding into the culture medium (10, 16, 18–20, 39). The unexpected presence of long fimbriae in the *A. oris srtA*-deficient cell surface rather than the culture medium suggests that the pilus-specific sortase enzymes SrtC1 and SrtC2 in *A. oris* might perform both functions of pilus assembly: Pilus polymerization and cell wall anchoring of pilus polymers. To test this hypothesis, we generated triple deletion mutants devoid of *gspA*, *srtA*, and *srtC1* (Δ*gspA*/Δ*srtA*/Δ*srtC1*) or *gspA*, *srtA*, and *srtC2* (Δ*gspA*/Δ*srtA*/Δ*srtC2*). The generated mutants were analyzed by using a pilus polymerization assay as describe previously (40), in which cell cultures were subjected to cell fractionation, and the culture medium (S) and cell wall (W) fractions were immunoblotted with antibodies specific against type 1 and type 2 fimbrial shaft (i.e., α-FimP and α-FimA, respectively). Results show that deletion of *srtA* in the Δ*gspA* strain did not cause any apparent defects of FimA and FimP assembly (Fig. 2 *A* and *B*, first 4 lanes). Deletion of *srtC1* in the Δ*gspA*/Δ*srtA* mutant strain abrogated polymerization of FimP (Fig. 2*A*, next 2 lanes), confirming the role of SrtC1 in pilus polymerization (30). Intriguingly, in the Δ*gspA*/Δ*srtA*/Δ*srtC2* triple mutant, in which SrtC1 is present, FimP pilus polymers were abundantly produced but mostly released into the culture medium (Fig. 2*A*, last 2 lanes). Independently, an analysis

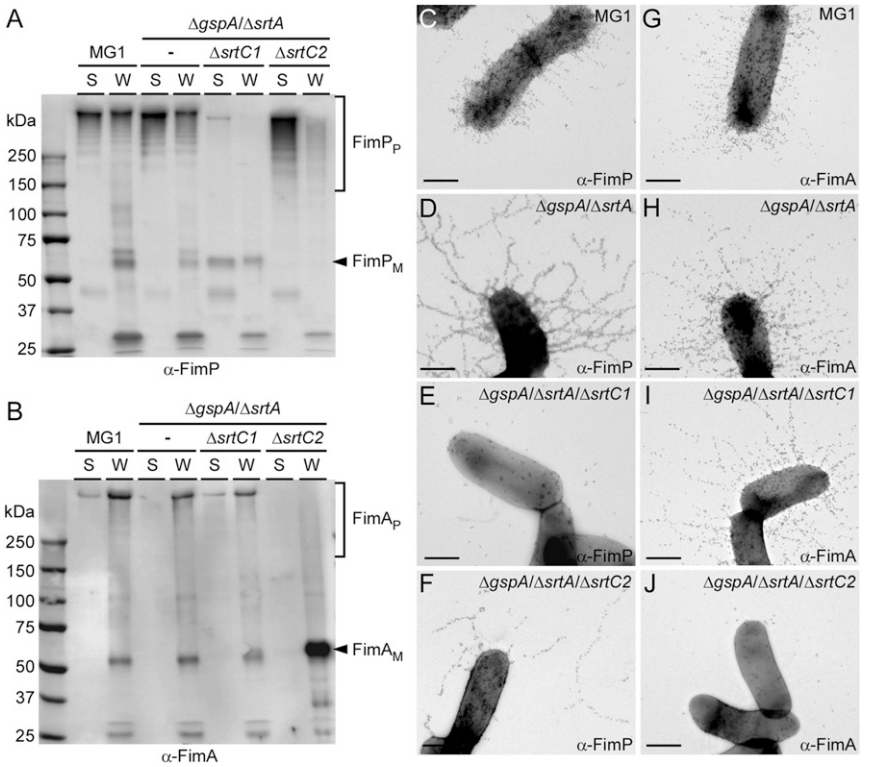

Fig. 2. Pilus-specific sortase SrtC2 possesses pilus polymerization and cell wall anchoring functions. (*A* and *B*) Culture medium (S) and cell wall (W) fractions of wild-type MG1, Δ*gspA*/Δ*srtA*, Δ*gspA*/Δ*srtA*/Δ*srtC1*, and Δ*gspA*/Δ*srtA*/Δ*srtC2* strains were analyzed by immunoblotting with α-FimP (*A*) or α-FimA (*B*). (*C–J*) The same set of strains were subjected to immunogold labeling, as described in Fig. 1, with α-FimP (*C–F*) or α-FimA (*G–J*). (Scale bars, 0.5 μm.)

of pilus assembly by IEM showed no detectable fimbriae in the Δ*gspA*/Δ*srtA*/Δ*srtC1* triple-mutant cell envelope, while detached fimbriae were found scattered around the Δ*gspA*/Δ*srtA*/Δ*srtC2* mutant cells (Fig. 2 *C–F*).

When the same set of samples used in Fig. 2*A* was immunoblotted with α-FimA, no significant defects in type 2 fimbrial assembly were observed in strains Δ*gspA*/Δ*srtA* and Δ*gspA*/Δ*srtA*/Δ*srtC1* when compared to the MG1 strain (Fig. 2*B*, first 6 lanes), while no type 2 pilus polymers were observed in the Δ*gspA*/Δ*srtA*/Δ*srtC*2 mutant (Fig. 2*B*, last 2 lanes). IEM analysis with α-FimA that revealed extensively long FimA fimbriae in strains Δ*gspA*/Δ*srtA* and Δ*gspA*/Δ*srtA*/Δ*srtC1*, but not in the Δ*gspA*/Δ*srtA*/Δ*srtC*2 mutant (Fig. 2 *G–J*). Collectively, these results confirm that SrtC1 and SrtC2 are specifically required for the polymerization of their cognate pilins. Most importantly, our results reveal that 1 of the 2 pilus pilus-specific sortases, SrtC2, is capable of anchoring both types of extended pilus polymers to the bacterial cell wall when the housekeeping sortase SrtA is absent.

The Housekeeping Sortase SrtA Determines the Optimal Pilus Length Required for Bacterial Coaggregation. The aberrant extension of CafA-containing pili in the Δ*srtA* mutant and the striking coaggregation defect of this mutant reported above suggest that the relative distance of CafA from the bacterial surface is crucial for cell-to-cell interactions. To probe this further, we sought to control pilus length by expressing *fimA* under the control of an inducible promoter (p*tetR*-R*-FimA) (34). Inducers were added to exponentially grown cultures and sampled at several time intervals for Western blotting, IEM, and coaggregation assays. As previously reported, the MG1 strain produced pilus polymers containing FimA and CafA retained in the cell wall fractions of exponential and overnight cell cultures (*SI Appendix*, Fig. S4*A*). In the Δ*fimA* mutant background, which lacks FimA and CafA polymers, induction of FimA for 3 h and overnight produced increasing FimA polymers as evident by the presence of the high molecular weight species above the 250-kDa marker especially in the overnight samples (*SI Appendix*, Fig. S4 *A*, *Left*). Immunoblotting of these same samples with α-CafA led to the same conclusion (*SI Appendix*, Fig. S4 *A*, *Right*). Independent analysis by IEM showed that induction of FimA also resulted in extension of FimA fimbriae and the increased distance of the CafA-tip from the cell envelope (*SI Appendix*, Fig. S4*B*); note that unlabeled fimbriae seen these samples are from type 1 fimbriae. Functionally, the induction of CafA-associated fimbriae resulted in increased in bacterial coaggregation, although it was not at the same level as seen with the wild-type cells, even when samples were grown overnight upon induction (*SI Appendix*, Fig. S4*C*). This partial concordance could be due to a variety of reasons, including a competition between SrtA and SrtC2 for FimA. To overcome this potential limitation and to obtain cells with long pili formed in the presence of SrtA, we engineered a vector that constitutively expressed both FimA and SrtC2. This plasmid expressed both FimA and SrtC2 as determined by Western blotting with antibodies against each protein in different cellular fractions. Compared to the wild-type and Δ*srtC2* strains without the recombinant plasmid, the levels of FimA and SrtC2 proteins increased considerably when the strains harbored the *fimA-srtC2* plasmid (*SI Appendix*, Fig. S5 *A* and *B*). Significantly, the plasmid led to the production of long pili (*SI Appendix*, Fig. S5*C*), comparable to those seen in the absence of SrtA, and also caused a pronounced defect in coaggregation (*SI Appendix*, Fig. S5*D*), akin to that observed with the SrtA-depleted strain. Clearly, elongated pili deter *Actinomyces* from undergoing interspecies interactions that normally take place in the oral cavity.

The preceding results invoke the hypothesis that a key function of the housekeeping sortase SrtA in *A. oris* is to control and generate a pilus length optimally suited for interspecies interactions.

To examine whether SrtA directly regulates pilus length, we cloned the *srtA* gene under the control of the same inducible promoter as described above (p*tetR*-R*-SrtA). We then analyzed exponential cultures of the Δ*gspA*/Δ*srtA* mutant containing this plasmid induced for various time points for SrtA expression, pilus assembly, and bacterial coaggregation. For SrtA expression, membrane fractions were isolated and immunoblotted with antibodies against SrtA (α-SrtA) or a control membrane protein, MdbA (α-MdbA). Fig. 3*A* shows that while no SrtA signal was detected in the Δ*gspA*/Δ*srtA* mutant, SrtA expression was steady in the MG1 strain during the first hour of culture. Addition of inducers resulted in progressively increased expression of SrtA (Fig. 3*A*). To visualize pili and CafA positioning, the Δ*gspA*/Δ*srtA*/p*tetR*-R*-SrtA strain culture was sampled at times 0, 60, and 120 min after induction and examined by IEM with α-FimA and α-CafA. As expected, induction of SrtA in the Δ*gspA*/Δ*srtA* mutant resulted in shortening of pilus length, hence CafA's relative distance from the cell envelope (Fig. 3*B*). We next analyzed the same set of cell cultures for bacterial coaggregation. Compared to the MG1 parent, induction of *srtA* in the Δ*gspA*/Δ*srtA* strain over time steadily enhanced coaggregation, unlike the Δ*fimA* and Δ*gspA*/Δ*srtA* mutants used as controls (Fig. 3*C*). Taken together, we conclude that the polymicrobial interactions in *A. oris* mediated by the coaggregation factor CafA require a proper presentation of this adhesin at the pilus tip of type 2 fimbriae, whose optimal length is controlled by the protein level of the housekeeping sortase SrtA.

Structure Determination Reveals That the Housekeeping Sortase SrtA of *A. oris* Is a Class E Sortase. To understand how SrtA functions as a regulator of pilus length, we determined the high-resolution X-ray crystal structure of its extracellular catalytic domain encompassing residues 78 to 257, which shares primary sequence homology to known sortase catalytic domains, but lacks the N-terminal transmembrane-anchoring segment. Crystals of the SrtA extracellular catalytic domain were obtained in space group $P2_1$ diffracting up to 1.7-Å resolution. They contain 4 essentially identical molecules in the asymmetric unit. The *A. oris* SrtA structure adopts a conserved "sortase" fold (41–43), composed of an 8-stranded β-barrel that is flanked by 5 α-helices (Fig. 4*A* and *SI Appendix*, Fig. S6*A*). Located at the top of the β-barrel, the SrtA active site structure is well conserved and formed by H148, C216, and R229 residues (Fig. 4*A*). While structurally similar to other members of the sortase superfamily, the SrtA core structure differs slightly as it contains a 4-residue insertion at the beginning of strand β2 that disrupts the β-sheet (*SI Appendix*, Fig. S6*B*). The insertion is formed by residues G106-V107-Thr108-Asn109 and causes the chain to protrude (*SI Appendix*, Fig. S6 *A* and *B*), a feature absent in the closest structural homologs of SrtA that have a smooth transition from their β1-β2 loops into the β2 strand. This unique protuberance in *A. oris* SrtA is positioned distal to the active site and its functional importance, if any, is not known.

Based on its primary sequence, SrtA is a member of the class E subfamily of sortases that predominate in Actinobacteria (21). At present, only 2 class E sortase structures have been determined, the *A. oris* SrtA structure reported here and the recently reported structure of the SrtE1 enzyme from *S. coelicolor* (PDB ID code 5CUW) (24). An analysis of the SrtA structure using DALI (44) reveals that it is most closely related to SrtE1; they have a *z*-score of 22.5 and their backbone coordinates can be superimposed with an rmsd of 1.6 Å (Fig. 4*B*). As compared to other members of the sortase superfamily, the structures of the class E SrtA and SrtE1 enzymes harbor distinct β3/β4 and β6/β7 loops that are positioned closer to one another. It is noteworthy that both enzymes contain a tyrosine residue located in the β3/β4 loop: That is, Y131 in *A. oris*, which in *S. coelicolor* has been implicated in the recognition of the LAETG motif (24). Notably, in both enzymes their β6/β7 loops have a 21-amino acid insertion that immediately follows the 3_{10} helix positioned adjacent to the active site cysteine. This long insertion is similar in length to that observed in class B sortases, but atypically is devoid of secondary structure, whereas class B sortases contain an additional α-helix. The unique class E loop insertion is evident when the *A. oris* SrtA structure is compared to that of the sortase SrtA enzyme from *Streptococcus pyogenes* (45) (PDB ID code 3FN5) (Fig. 4*C*). This class A enzyme exhibits a high degree of structural similarity to *A. oris* SrtA (*z*-score 19.1 and backbone rmsd of 2.1 for 161 corresponding residues), but it lacks the β6/β7 loop insertion. Furthermore, the *A. oris* SrtA does not have a lid motif first observed in the class C sortase enzymes (8), such as *Streptococcus pneumoniae* SrtC1 (46) and *A. oris* SrtC1 (PDB ID code 2XWG) (47) (Fig. 4*D*).

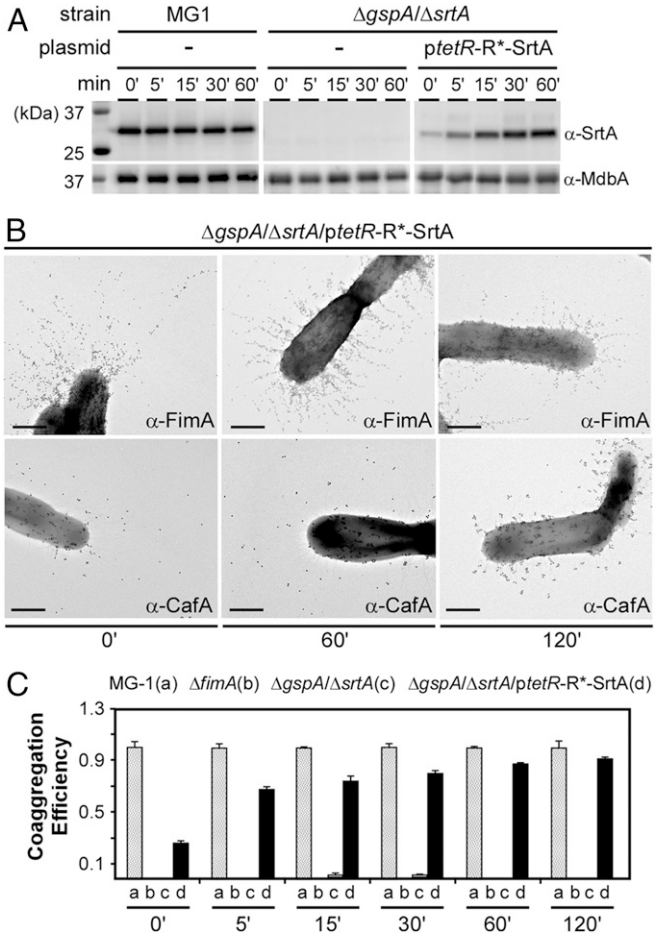

Fig. 3. Intracellular levels of SrtA affect pilus length and bacterial coaggregation. (*A*) MG1, Δ*gspA*/Δ*srtA*, and this mutant expressing *srtA* under the control of an inducible promoter and a riboswitch element (p*tetR*-R*-SrtA) were used in this experiment. Next, 100 ng/mL anhydrotetracycline (AHT) and 1 mM theophylline were added to each bacterial culture, and at various time points of induction, aliquots of bacterial cultures were removed, normalized to equivalent cell density, and subjected to mutanolysin treatment to generate protoplasts. Protein samples from protoplasts were analyzed by SDS/PAGE and immunoblotted with specific antibodies against SrtA and MdbA; the latter is a membrane protein used as a control. (*B*) Culture aliquots of the Δ*gspA*/Δ*srtA* mutant carrrying p*tetR*-R*-SrtA at indicated time points were subjected to IEM using α-FimA and α-CafA, followed by goat anti-rabbit IgG conjugated to 12- and 18-nm gold particles, respectively. (Scale bars, 0.5 μm.) (*C*) Aliquots of indicated cultures (annotated in letters) at various time points were subjected to a quantitative coaggregation assay that measures coaggregation efficiency of each strain relative to MG1. The results are representative of 3 independent experiments performed in triplicate. Note that the Δ*fimA* and Δ*gspA*/Δ*srtA* mutants were unable to mediate bacterial coaggregation.

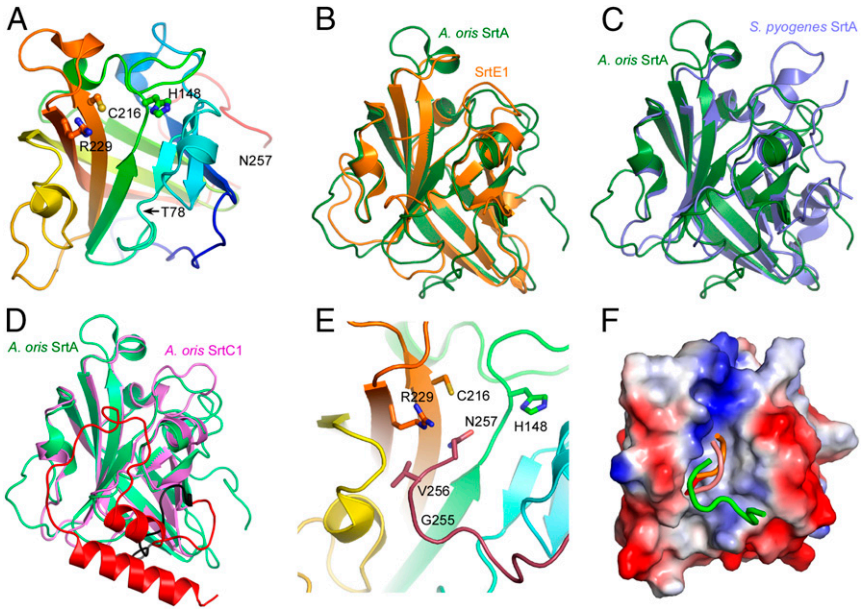

Fig. 4. Determination of SrtA structures. (*A*) The crystal structure of an SrtA molecule consisted of residues 71 to 257 was determined to 1.7-Å resolution by X-ray crystallization. The catalytic residues H148, C216, and R229 are highlighted. (*B–D*) The *A. oris* SrtA structure is compared to the structure of *S. coelicolor* SrtE1 (PDB ID code 5CUW), *S. pyogenes* SrtA (PDB ID code 3FN5), and *A. oris* SrtC1 (PDB ID code 2XWG). The lid region of *A. oris* SrtC1, absent in *A. oris* SrtA, is highlighted in red. (*E*) The asymmetric unit of SrtA crystal packaging the C-terminal GVN tripeptide from monomer A is seen in the active site of monomer A. (*F*) Shown is electrostatic potential surface for monomer A (blue is positive charge; red is negative). The C terminus of monomer B is shown as green. Red, orange, and beige represent substrates in structures 1T2W, 2KID, and 2RUI, respectively.

A remarkable feature in the *A. oris* SrtA crystal packaging is that in the asymmetric unit SrtA molecules are positioned such that residues in the β5/β6 loop and C-terminal extension of 1 molecule pack against residues within the β7/β8 loop and sorting signal binding of an adjacent protein, respectively (Fig. 4 *E* and *F* and *SI Appendix*, Fig. S6*C*). These contacts bury 770 Å^2 of solvent surface area and are primarily formed by hydrophilic residues. Interprotein contacts originating from the C-terminal extension are intriguing, as they partially occlude the cell wall sorting-signal binding site. The C-terminal extension, 16 amino acids in length, follows strand β8, and approaches the adjacent enzyme near its catalytically essential Arg229 residue (*SI Appendix*, Fig. S6*C*), projecting its C-terminal Gly255-Val256-Asn257 (GVN) residues in between helix H2 and the β6/β7 loop. Interestingly, the GVN tripeptide is positioned in a similar manner as an ANA tripeptide found in the active site pocket of the structure of the *S. coelicolor* sortase SrtE1 (24). The ANA peptide presumably corresponds to Ala168-Ala170 in the unstructured N-terminal linker of SrtE1 that precedes the catalytic domain, and its binding to the active site has been proposed to emulate that of the sorting signal substrate (24). Based on modeling studies and experimentally determined structures of sortase-substrate complexes, this region on the enzyme is believed to form a recognition subsite for the leucine and alanine residues within LAXTG sorting signal. Intriguingly, the valine residue within the C-terminal GVN sequence is packed against helix H4 located in the β6/β7 loop, such that it occupies the predicted subsite for the leucyl side chain within the sorting signal (Fig. 4*E* and *SI Appendix*, Fig. S6*C*). Extrapolating this structural feature to SrtA on the cell surface, it seems plausible that interprotein interactions mediated by C-terminal residues within the enzymes could alter activity by modulating substrate binding.

Two Conserved Structural Elements of *A. oris* SrtA Modulate Pilus Length and Bacterial Coaggregation. To assess the role of the GVN tripeptide and Y131 in SrtA functionality, we generated recombinant plasmids that express SrtA mutants with Y131A substitution, deletion of GVN (ΔGVN), replacement of GVN by alanine (3A), or combination of both mutations (Y131A/ΔGVN). For functional studies here, we chose to test the individual plasmids in an *srtA* suppressor mutant, Δ*lcp*/Δ*srtA*, which was selected to disable the glycosylation step of GspA and hence prevent its toxicity (34, 48). An analysis of membrane fractions of the transformed strains by immunoblotting established that none of the mutations affected SrtA expression and instability (Fig. 5*A*). Next, the IEM analysis using antibodies against both types of fimbriae showed that the suppressor strain Δ*lcp*/Δ*srtA* produced long polymers of both pilus types, with CafA signal detected farther away from the cell surface as compared to the MG1 strain (Fig. 5*B*; panel sets MG1 and Δ*lcp*/Δ*srtA*, top to bottom). Ectopic expression of *srtA* in the double mutant returned the pilus length to the level similar to the MG1 parent (Fig. 5*B*, panel set Δ*lcp*/Δ*srtA*/pSrtA). In contrast, the SrtA-Y131A mutant assembled fimbriae with shorter length as compared to the MG1 and SrtA complementing strains (Fig. 5*B*, panel set Δ*lcp*/Δ*srtA*/Y131A), while each of the *srtA* mutants, ΔGVN, 3A, and Y131A/ΔGVN, produced long fimbriae as observed in the case of the suppressor strain Δ*lcp*/Δ*srtA* (Fig. 5*B*; compare the second panel set to the last 3 panel sets). Strikingly, the Y131A mutant exhibited a minor coaggregation defect (small clumps of cells) as compared to the MG1 and the complemented Δ*lcp*/Δ*srtA*/pSrtA strains (Fig. 5*C*, first 3 circles), whereas the ΔGVN, 3A, and Y131A/ΔGVN mutants were all unable to coaggregate with *S. oralis* (Fig. 5*C*, last 3 circles).

The differential pilus length and coaggregation phenotypes described in Fig. 5 above raised the possibility that mutations of Y131 and the loop might shift the activity of SrtA toward nonpilin substrates, particularly the highly expressed cell wall-anchored GspA protein (34). To examine this potential competition, we characterized the SrtA mutants in the strain lacking both *srtA* and *gspA* (Δ*gspA*/Δ*srtA*) for their proficiency in pilus assembly and bacterial coaggregation. Strikingly, while cells of the Δ*gspA*/Δ*srtA* mutant expressing SrtA with Y131A mutation

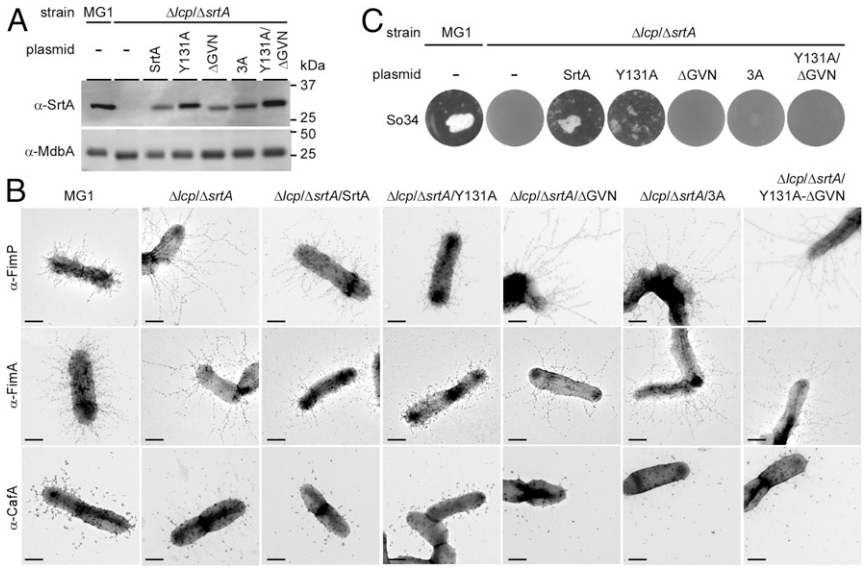

Fig. 5. Pilus shortening and elongation are modulated by SrtA structural elements. (*A*) Protoplast fractions of the MG1, Δ*lcp*/Δ*srtA*, and this mutant expressing wild-type SrtA or its variants were subjected to immunoblotting with α-SrtA and α-MdbA. The same set of *A. oris* strains in *A* were analyzed for pilus assembly by IEM using α-FimP, α-FimA, and α-CafA (*B*) and coaggregation with *S. oralis* So34 (*C*). (Scale bars, 0.5 μm.)

still produced short FimA fimbriae and exhibited a coaggregation defect, the strain Δ*gspA*/Δ*srtA* expressing mutant SrtA with GVN loop deletion assembled FimA fimbriae in lengths comparable to that produced by the Δ*gspA*/Δ*srtA*/pSrtA and displayed a coaggregation-positive phenotype (*SI Appendix*, Fig. S7), in sharp contrast with the phenotype of this same sortase mutant expressed in the Δ*lcp*/Δ*srtA* background (Fig. 5). Evidently, a pilus length-determining attribute is inherent and encoded genetically in the structure of the *A. oris* housekeeping sortase that acts in concert with the vital function of the enzyme in anchoring numerous other surface proteins to the cell wall.

Discussion

The concept of the importance of spatial positioning of bacterial adhesins displayed at a pilus tip that promotes long-distance attachment has been proposed for some time in gram-positive bacteria (5, 49). In this work, we provide experimental evidence that coaggregation between oral biofilm bacteria mediated by the pilus tip adhesin CafA in *A. oris* requires an optimal pilus length. Furthermore, we demonstrate that the housekeeping sortase SrtA acts to control the length of both pilus types produced by this bacterium. This revelation resulted from a somewhat unexpected but striking observation that *A. oris* mutant strains devoid of *srtA* assemble uncharacteristically long pili on the cell surface that fail to mediate bacterial coaggregation (Fig. 1 and *SI Appendix*, Fig. S1) (34). Our systematic analysis of this phenomenon showed that the coaggregation defect was not due to a defect in the major coaggregation factor CafA since the *srtA* deletion mutant (Δ*gspA*/Δ*srtA*) and its complemented derivative (Δ*gspA*/Δ*srtA*/pSrtA) expressed the same level of surface CafA (*SI Appendix*, Fig. S1). We then established that an optimal pilus length is critical for bacterial coaggregation by providing 2 important pieces of contrasting evidence. First, inducible expression of SrtA in the Δ*gspA*/Δ*srtA* mutant shortened the length of aberrantly long pili produced in the absence of SrtA and restored positive coaggregation (Fig. 3). Second, by varying the expression of the major pilus shaft FimA in various strain background, we were able to manipulate the length of the pilus and demonstrate that coaggregation efficiency varied depending on whether the pili were short, long, or of an optimally suited length that is produced by the wild-type. (*SI Appendix*, Figs. S4 and S5).

The findings above, however, pose 2 related conundrums: How pilus polymers are anchored to the cell wall without the housekeeping sortase SrtA, whose known function is to join the pilus to bacterial peptidoglycan, and how SrtA alters pilus polymerization, which is known to be dependent on the pilus-specific sortase SrtC2 (9). It is noteworthy that in many gram-positive bacteria, the housekeeping sortase enzymes are required to carry out the cell wall-anchoring step (10, 16, 18–20), although some pilus-specific sortase enzymes, such as those in *C. diphtheriae*, can perform this function, albeit at a lower efficiency (16). Our results (Fig. 2) revealed that SrtC2, the type 2 pilus-specific sortase, is capable of anchoring both type 1 and 2 pilus polymers to the cell wall quite efficiently. It follows that in the absence of SrtA, SrtC2 continues to polymerize FimA pilins in an uninterrupted fashion, leading to aberrant extension of pilus polymers, until most FimA pilins are consumed. With few FimA available for polymerization, cell wall anchoring of pili by SrtC2 is favored. In contrast, in the presence of SrtA, SrtC2 and SrtA enzymes compete for the same substrate FimA, while SrtA also binds to and attaches many other surface proteins to the cell wall. Indeed, increased expression of SrtA shifts the reaction stoichiometry toward cell wall anchoring of pilus polymers, resulting in shortened pili (Fig. 3).

An interesting question is how SrtA recognizes different substrates and carries out the balanced enzymatic reactions that result in cell wall anchoring of surface proteins and pilus polymers with optimal length for bacterial coaggregation. Our crystallization studies revealed that SrtA is a class E sortase, whose substrates are predicted to contain a LAXTG motif (21, 24); SrtA harbors 2 conserved features characteristic of this class of enzymes: Y131 and the GVN motif (Fig. 4). Previous studies revealed that the *A. oris* genome encodes 18 surface proteins, the majority of which, including GspA, have the LAXTG motif. Based on the results in Fig. 5 and *SI Appendix*, Fig. S6, which showed that the *A. oris* strain carrying the Y131A mutation assembles pili that are shorter than the parental strain, we propose that this residue plays a critical regulatory role in the recognition of the LAXTG motif. The Y131A mutation shifts the SrtA reactivity toward the LPXTG motif, which is present in all the pilus proteins. As a result, pilus polymerization is aborted by SrtA-mediated cell wall anchoring of the resulting polymers, leading

to the shortened pili. When the GVN motif of SrtA is mutated, however, long pili are generated when GspA is present (i.e., in the Δ*lcp*/Δ*srtA* strain). We surmise that the GVN mutations augment the reactivity of SrtA toward GspA, a highly expressed glycoprotein that accumulates in the membrane in toxic levels when *srtA* is deleted (34). This increased affinity for LAXTG-containing substrates makes SrtA less available for cell wall anchoring of pilus polymers, thus permitting SrtC2 to continue to polymerize FimA pilins and form extremely long pili (Fig. 6). This scenario lends support from the fact that when the same GVN mutant was tested in the Δ*gspA*/Δ*srtA* mutant, normal-length pili were produced and efficient coaggregation was observed (*SI Appendix*, Fig. S7).

In conclusion, we have uncovered 2 key structural elements within the housekeeping sortase SrtA of *A. oris* that govern its specificity toward the 2 types of protein substrates that this enzyme links to the bacterial cell wall. The identified elements coordinate the balanced stoichiometry of pilus polymerization and cell wall anchoring of pilus polymers, leading to an optimal spatial positioning of the coaggregation factor CafA that is essential for polymicrobial interactions involving *A. oris*. Many aspects of the molecular basis of cell-to-cell interactions and interspecies communications still remain elusive. Because pili are pivotal in these processes and the overall mechanism of cell wall anchoring of pili is conserved, the paradigm presented here provides a footprint for the studies of pilus assembly in gram-positive bacteria in general.

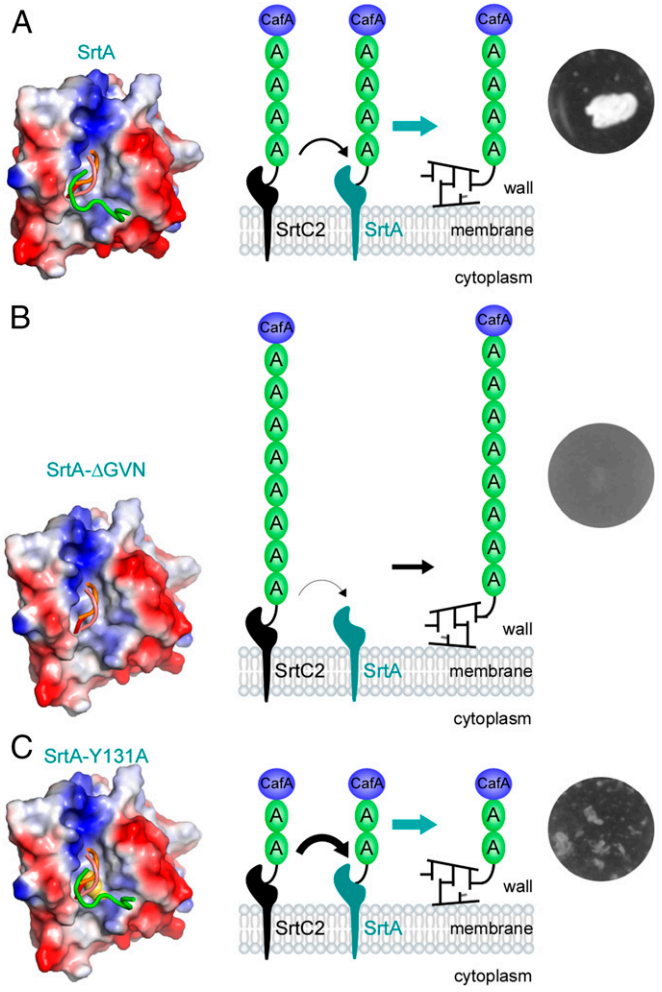

Fig. 6. (*A*–*C*) A model of pilus polymerization and cell wall anchoring modulated by activities of pilus-specific sortase and the housekeeping sortase. See *Discussion* for details; A131 is highlighted in yellow.

Materials and Methods

Bacterial Strains, Plasmids, Media, and Cell Culture. Bacterial strains and plasmids used in this study are recorded in *SI Appendix*, Tables S1 and S2. *SI Appendix, SI Materials and Methods* also contains pertinent information regarding genetics, biochemical assays, protein purification, and structural determination. *Actinomyces* strains were grown in heart infusion broth or on heart infusion agar plates at 37 °C and 5% CO_2. Streptococci were grown in brain heart infusion supplemented with 1% glucose in an anaerobic chamber. *Escherichia coli* DH5α, used for molecular cloning experiments, was grown in Luria-Broth (LB) at 37 °C. When required, antibiotics (kanamycin or streptomycin) were added into medium at a final concentration of 50 μg mL^{-1}. For the tetracycline/riboswitch inducible system, anhydrotetracycline and theophylline were added to culture at 100 ng mL^{-1} and 1 mM, respectively. Reagents were purchased from Sigma unless indicated otherwise.

Electron Microscopy. Negative staining and immunogold labeling (IEM) of *A. oris* cells were performed according to a previously published protocol (50). Briefly, for negative staining a drop of bacterial suspension in PBS was placed onto carbon-coated nickel grids and stained with 1% uranyl acetate. Samples were examined using a JEOL JEM1400 electron microscope. For immunogold-labeling of pili, bacterial cells on grids were first stained with specific antibodies against *A. oris* pilins (i.e., α-FimA, α-FimP, and α-CafA [1:100 dilution]), followed by staining with IgG-conjugated gold particles and 1% uranyl acetate. Antibody specificity was previously determined in prior studies (9, 29, 30, 32).

Estimation of Pilus Length by IEM and Cryo-ET. Pilus length in *A. oris* was estimated by IEM as follows. After the IEM procedure of MG1 and Δ*gspA*/Δ*srtA* strains, electron micrographs of cells labeled with anti-CafA antibodies were taken. A circumferential outline of CafA-labeled gold particles was drawn. The linear distances between the outline and the cell envelope at various locations were determined by ImageJ (https://imagej.nih.gov/ij/). For each cell, 20 measurements were collected and 10 cells were used for each strain.

For cryo-ET analysis, bacterial pellets were suspended in PBS and mixed with 10-nm gold particles (ratio of 1:10 vol/vol). Cell suspensions (5 μL) were applied onto a glow-discharged Quantifoil grid for 1 min. The grid was blotted with filter papers and plunge-frozen into liquid ethane using a gravity-driven plunger apparatus. The resulting frozen-hydrated specimens were imaged at −170 °C using a Polara G2 electron microscope (FEI Company) equipped with a field-emission gun and a Direct Detection Camera (Gatan K2 Summit). SerialEM (51) was used to collect low-dose, single-axis tilt series with a dose fractionation mode at 15-μm defocus. For the wild-type MG1, the microscope was operated at 300 kV with a magnification of 9,400×. The effective pixel size was 8.4 Å after 2 × 2 binning. A cumulative electron dose of ∼100 e^{-}/Å ^{2} was distributed over 35 images covering an angular range from −51° to +51° with an angular increment of 3°. For the Δ*gspA*/Δ*srtA* mutant, the magnification of 4,700× was used for visualizing long pili with the effective pixel size of 16.5 Å after 2 × 2 binning. Images were collected at higher defocus (∼20 μm). The total electron dose was ∼100 e^{-}/Å ^{2}, distributed over 52 images and covering an angular range of −51° to +51°, with an angular increment of 2°.

The tomographic data were analyzed as previously described (52, 53). Briefly, the MotionCorr package was used for drift correction of dose-fractionated data (54). The tomographic tilt series were aligned and reconstructed by IMOD (38). For the length estimation of pili, IMOD was employed to manually depict point by point along pili. All coordinates of collected points were used to estimate pilus length. In total, 10 pili in wild-type cells from 5 tomograms and 10 pili in mutant cells from 4 tomograms were analyzed, respectively.

All statistical analysis was performed using GraphPad Prism 5.0 as previously reported, with significant differences determined using the unpaired *t* test with Welch's correction and a nonparametric, 2-tailed value for *P* of ≤0.05, ≤0.01, or 0.001 considered significant (55).

SrtA Structure Determination. Experimental details regarding protein purification and crystallization of SrtA, as well as data collection, structure determination, and refinement, are described in *SI Appendix, SI Materials and Methods*.

Atomic coordinates and structure factors were deposited into the Protein Data Bank with ID code 5UTT.

ACKNOWLEDGMENTS. We thank Jun Liu (Yale University) for technical assistance, our laboratory members for critical review of the manuscript and discussion, and all members of the Structural Biology Center at Argonne National Laboratory for their help in conducting X-ray diffraction data collection. Argonne is operated by UChicago Argonne, LLC for the US Department of Energy, Office of Biological and Environmental Research under Contract DE-AC02-06CH11357. This work was also supported by funds from the National Institute of Allergy and Infectious Diseases, National Institutes of Health, Department of Health and Human Services, under Contracts HHSN272201200026C and HHSN272201700060C (to A.J.); and the National Institute of Dental and Craniofacial Research (NIDCR)/NIH under Awards DE017382 (to H.T.-T.) and DE026574 (to C.W.). S.D.S. was supported by NIDCR under Award F31-DE027295 and the Kopchick fellowship from MD Anderson University of Texas Health, Graduate School of Biomedical Sciences.

1. M. K. Hospenthal, T. R. D. Costa, G. Waksman, A comprehensive guide to pilus biogenesis in Gram-negative bacteria. *Nat. Rev. Microbiol.* **15**, 365–379 (2017).
2. C. Danne, S. Dramsi, Pili of gram-positive bacteria: Roles in host colonization. *Res. Microbiol.* **163**, 645–658 (2012).
3. Z. A. McGee, R. R. Dourmashkin, J. G. Gross, J. B. Clark, D. Taylor-Robinson, Relationship of pili to colonial morphology among pathogenic and nonpathogenic species of Neisseria. *Infect. Immun.* **15**, 594–600 (1977).
4. F. Yoshimura, Y. Murakami, K. Nishikawa, Y. Hasegawa, S. Kawaminami, Surface components of *Porphyromonas gingivalis*. *J. Periodontal Res.* **44**, 1–12 (2009).
5. A. Mandlik, A. Swierczynski, A. Das, H. Ton-That, Pili in Gram-positive bacteria: Assembly, involvement in colonization and biofilm development. *Trends Microbiol.* **16**, 33–40 (2008).
6. D. J. Echelman *et al*., CnaA domains in bacterial pili are efficient dissipaters of large mechanical shocks. *Proc. Natl. Acad. Sci. U.S.A.* **113**, 2490–2495 (2016).
7. H. Ton-That, O. Schneewind, Assembly of pili on the surface of *Corynebacterium diphtheriae*. *Mol. Microbiol.* **50**, 1429–1438 (2003).
8. S. D. Siegel, J. Liu, H. Ton-That, Biogenesis of the Gram-positive bacterial cell envelope. *Curr. Opin. Microbiol.* **34**, 31–37 (2016).
9. A. Mishra, A. Das, J. O. Cisar, H. Ton-That, Sortase-catalyzed assembly of distinct heteromeric fimbriae in *Actinomyces naeslundii*. *J. Bacteriol.* **189**, 3156–3165 (2007).
10. J. M. Budzik, L. A. Marraffini, O. Schneewind, Assembly of pili on the surface of *Bacillus cereus* vegetative cells. *Mol. Microbiol.* **66**, 495–510 (2007).
11. S. R. Nallapareddy *et al*., Endocarditis and biofilm-associated pili of *Enterococcus faecalis*. *J. Clin. Invest.* **116**, 2799–2807 (2006).
12. S. Dramsi *et al*., Assembly and role of pili in group B streptococci. *Mol. Microbiol.* **60**, 1401–1413 (2006).
13. M. Mora *et al*., Group A *Streptococcus* produce pilus-like structures containing protective antigens and Lancefield T antigens. *Proc. Natl. Acad. Sci. U.S.A.* **102**, 15641–15646 (2005).
14. R. Rosini *et al*., Identification of novel genomic islands coding for antigenic pilus-like structures in *Streptococcus agalactiae*. *Mol. Microbiol.* **61**, 126–141 (2006).
15. A. L. Nelson *et al*., RrgA is a pilus-associated adhesin in *Streptococcus pneumoniae*. *Mol. Microbiol.* **66**, 329–340 (2007).
16. A. Swaminathan *et al*., Housekeeping sortase facilitates the cell wall anchoring of pilus polymers in *Corynebacterium diphtheriae*. *Mol. Microbiol.* **66**, 961–974 (2007).
17. J. M. Budzik, S. Y. Oh, O. Schneewind, Cell wall anchor structure of BcpA pili in *Bacillus anthracis*. *J. Biol. Chem.* **283**, 36676–36686 (2008).
18. H. V. Nielsen *et al*., Pilin and sortase residues critical for endocarditis- and biofilm-associated pilus biogenesis in *Enterococcus faecalis*. *J. Bacteriol.* **195**, 4484–4495 (2013).
19. A. H. Nobbs *et al*., Sortase A utilizes an ancillary protein anchor for efficient cell wall anchoring of pili in *Streptococcus agalactiae*. *Infect. Immun.* **76**, 3550–3560 (2008).
20. J. Sillanpää *et al*., Contribution of individual Ebp Pilus subunits of *Enterococcus faecalis* OG1RF to pilus biogenesis, biofilm formation and urinary tract infection. *PLoS One* **8**, e68813 (2013).
21. T. Spirig, E. M. Weiner, R. T. Clubb, Sortase enzymes in Gram-positive bacteria. *Mol. Microbiol.* **82**, 1044–1059 (2011).
22. S. Dramsi, P. Trieu-Cuot, H. Bierne, Sorting sortases: A nomenclature proposal for the various sortases of Gram-positive bacteria. *Res. Microbiol.* **156**, 289–297 (2005).
23. S. K. Mazmanian, G. Liu, H. Ton-That, O. Schneewind, *Staphylococcus aureus* sortase, an enzyme that anchors surface proteins to the cell wall. *Science* **285**, 760–763 (1999).
24. M. D. Kattke *et al*., Crystal structure of the *Streptomyces coelicolor* sortase E1 transpeptidase provides insight into the binding mode of the novel class E sorting signal. *PLoS One* **11**, e0167763 (2016).
25. A. Mandlik, A. Das, H. Ton-That, The molecular switch that activates the cell wall anchoring step of pilus assembly in gram-positive bacteria. *Proc. Natl. Acad. Sci. U.S.A.* **105**, 14147–14152 (2008).
26. H. Ton-That, L. A. Marraffini, O. Schneewind, Sortases and pilin elements involved in pilus assembly of *Corynebacterium diphtheriae*. *Mol. Microbiol.* **53**, 251–261 (2004).
27. H. J. Kang, F. Coulibaly, F. Clow, T. Proft, E. N. Baker, Stabilizing isopeptide bonds revealed in gram-positive bacterial pilus structure. *Science* **318**, 1625–1628 (2007).
28. O. Schneewind, D. M. Missiakas, Protein secretion and surface display in Gram-positive bacteria. *Philos. Trans. R. Soc. Lond. B Biol. Sci.* **367**, 1123–1139 (2012).
29. M. E. Reardon-Robinson *et al*., Pilus hijacking by a bacterial coaggregation factor critical for oral biofilm development. *Proc. Natl. Acad. Sci. U.S.A.* **111**, 3835–3840 (2014).
30. C. Wu *et al*., Dual function of a tip fimbrillin of *Actinomyces* in fimbrial assembly and receptor binding. *J. Bacteriol.* **193**, 3197–3206 (2011).
31. R. J. Gibbons, D. I. Hay, J. O. Cisar, W. B. Clark, Adsorbed salivary proline-rich protein 1 and statherin: Receptors for type 1 fimbriae of *Actinomyces viscosus* T14V-J1 on apatitic surfaces. *Infect. Immun.* **56**, 2990–2993 (1988).
32. A. Mishra *et al*., The *Actinomyces oris* type 2 fimbrial shaft FimA mediates coaggregation with oral streptococci, adherence to red blood cells and biofilm development. *Mol. Microbiol.* **77**, 841–854 (2010).
33. H. Ton-That, A. Das, A. Mishra, "Actinomyces oris Fimbriae: An adhesive principle in bacterial biofilms and tissue tropism" in *Genomic Inquiries into Oral Bacterial Communities*, P. E. Kolenbrander, Ed. (ASM Press, Washington, DC, 2011), chap. 4, pp. 63–77.
34. C. Wu *et al*., Lethality of sortase depletion in *Actinomyces oris* caused by excessive membrane accumulation of a surface glycoprotein. *Mol. Microbiol.* **94**, 1227–1241 (2014).
35. C. Wu *et al*., Structural determinants of *Actinomyces* sortase SrtC2 required for membrane localization and assembly of type 2 fimbriae for interbacterial coaggregation and oral biofilm formation. *J. Bacteriol.* **194**, 2531–2539 (2012).
36. M. M. Broadway *et al*., Pilus gene pool variation and the virulence of *Corynebacterium diphtheriae* clinical isolates during infection of a nematode. *J. Bacteriol.* **195**, 3774–3783 (2013).
37. S. D. Siegel, C. Wu, H. Ton-That, A type I signal peptidase is required for pilus assembly in the Gram-positive, biofilm-forming bacterium *Actinomyces oris*. *J. Bacteriol.* **198**, 2064–2073 (2016).
38. J. R. Kremer, D. N. Mastronarde, J. R. McIntosh, Computer visualization of three-dimensional image data using IMOD. *J. Struct. Biol.* **116**, 71–76 (1996).
39. L. Lalioui *et al*., The SrtA Sortase of *Streptococcus agalactiae* is required for cell wall anchoring of proteins containing the LPXTG motif, for adhesion to epithelial cells, and for colonization of the mouse intestine. *Infect. Immun.* **73**, 3342–3350 (2005).
40. A. Mishra *et al*., Two autonomous structural modules in the fimbrial shaft adhesin FimA mediate *Actinomyces* interactions with streptococci and host cells during oral biofilm development. *Mol. Microbiol.* **81**, 1205–1220 (2011).
41. B. Khare *et al*., Structural differences between the *Streptococcus agalactiae* housekeeping and pilus-specific sortases: SrtA and SrtC1. *PLoS One* **6**, e22995 (2011).
42. U. Ilangovan, H. Ton-That, J. Iwahara, O. Schneewind, R. T. Clubb, Structure of sortase, the transpeptidase that anchors proteins to the cell wall of *Staphylococcus aureus*. *Proc. Natl. Acad. Sci. U.S.A.* **98**, 6056–6061 (2001).
43. R. Zhang *et al*., Structures of sortase B from *Staphylococcus aureus* and *Bacillus anthracis* reveal catalytic amino acid triad in the active site. *Structure* **12**, 1147–1156 (2004).
44. L. Holm, P. Rosenström, Dali server: Conservation mapping in 3D. *Nucleic Acids Res.* **38**, W545–W549 (2010).
45. P. R. Race *et al*., Crystal structure of *Streptococcus pyogenes* sortase A: Implications for sortase mechanism. *J. Biol. Chem.* **284**, 6924–6933 (2009).
46. C. Manzano, T. Izoré, V. Job, A. M. Di Guilmi, A. Dessen, Sortase activity is controlled by a flexible lid in the pilus biogenesis mechanism of gram-positive pathogens. *Biochemistry* **48**, 10549–10557 (2009).
47. K. Persson, Structure of the sortase AcSrtC-1 from *Actinomyces oris*. *Acta Crystallogr. D Biol. Crystallogr.* **67**, 212–217 (2011).
48. S. D. Siegel *et al*., Structure and mechanism of LcpA, a phosphotransferase that mediates glycosylation of a Gram-positive bacterial cell wall-anchored protein. *MBio* **10**, e01580-18 (2019).
49. A. Mandlik, A. Swierczynski, A. Das, H. Ton-That, *Corynebacterium diphtheriae* employs specific minor pilins to target human pharyngeal epithelial cells. *Mol. Microbiol.* **64**, 111–124 (2007).
50. C. Chang, I. H. Huang, A. P. Hendrickx, H. Ton-That, Visualization of Gram-positive bacterial pili. *Methods Mol. Biol.* **966**, 77–95 (2013).
51. D. N. Mastronarde, Automated electron microscope tomography using robust prediction of specimen movements. *J. Struct. Biol.* **152**, 36–51 (2005).
52. B. Hu, W. Margolin, I. J. Molineux, J. Liu, The bacteriophage t7 virion undergoes extensive structural remodeling during infection. *Science* **339**, 576–579 (2013).
53. B. Hu *et al*., Visualization of the type III secretion sorting platform of *Shigella flexneri*. *Proc. Natl. Acad. Sci. U.S.A.* **112**, 1047–1052 (2015).
54. X. Li *et al*., Electron counting and beam-induced motion correction enable near-atomic-resolution single-particle cryo-EM. *Nat. Methods* **10**, 584–590 (2013).
55. T. T. Luong *et al*., Structural basis of a thiol-disulfide oxidoreductase in the hedgehog-forming actinobacterium *Corynebacterium matruchotii*. *J. Bacteriol.* **200**, e00783-17 (2018).